European Review for Medical and Pharmacological Sciences 2019; 23: 7619-7627

Knocking down PFL can improve myocardial ischemia/reperfusion injury in rats by up-regulating heat shock protein-20

R.-L. YIN, H. YOU, Y.-M. WU, F.-L. YE, W.-X. GU, J. SHEN

Department of Cardiology, the Wujiang Affiliated Hospital of Nantong Univ[illegible]y, Suzh[illegible]u, China

Abstract. – OBJECTIVE: To investigate the effect and mechanism of long non-coding ribonucleic acid (lncRNA) PFL on myocardial ischemia/reperfusion (I/R) injury in rats, and to provide a reference for the prevention and treatment of myocardial infarction (MI) in clinic.

MATERIALS AND METHODS: According to the random number table, 60 male Sprague-Dawley (SD) rats were randomly divided into 3 groups: Control group (n=20), I/R group (n=20), and I/R + PFL small interfering ribonucleic acid (siRNA) group (n=20). The I/R model was established by ligating the left anterior descending coronary artery (LAD) and then recanalizing it. PFL siRNAs were injected intravenous[ly] the tail vein of rats in I/R + PFL siRNA [gr]oup to construct a PFL knockout model. Trip[henyl] tetrazolium chloride (TTC) test was used to [de]tect the infarction area of each group. Echo[cardi]ography was adopted to measure the ejectio[n] fraction [EF (%)] and fraction s[hortening] [FS (%)] of rats in each group. Hem[atoxyl]in and eosin (H&E) staining was applied to dete[ct] the morphological changes in myocardial c[ells] each group. Terminal deoxynucleotidyl [tran]sferase dUTP nick end labeling (TU[NEL] staining was conducted to detect the apoptosis levels of myocardial cells and fibroblasts in heart tissues in each group. Meanwhile, the protein expression levels of apoptosis-related genes, Bcl-2-associated X protein (BAX), and Bcl-2, were measured via Western blotting. Also, the expression level of heat shock protein 20 (HSP-20) in the heart of three groups of rats was examined using immunohistochemistry staining. Finally, the effects of PFL siRNAs on the expression level of HSP-20 were detected via Western blotting.

RESULTS: PFL siRNAs could significantly improve I/R-induced cardiac insufficiency in rats, thus increasing EF (%) and FS (%) ($p<0.05$). Besides, PFL siRNAs could remarkably inhibit the infarction caused by I/R injury and reduce the infarction area from (59.54±3.45)% to (24.85±1.30)% ($p<0.05$). H&E staining results suggested that, compared with those in I/R group, the cardiac myofilament was better in alignment, degradation and necrosis were milder, and cell edema was notably reduced in I/R + PFL siRNA group. Immunohistochemistry and Western blotting results showed that PFL siRNAs could remarkably reverse the decrease in the HSP-20 expression caused by I/R ($p<0.05$).

CONCLUSIONS: We found that PFL knockdown can significantly improve the myocardial injury caused by I/R and improve the cardiac function in rats. The mechanism may be related to the activation of HSP-20 by PFL siRNAs. Therefore, PFL is expected to become a new target for the treatment of MI.

Key words:
Myocardial ischemia/reperfusion, LncRNA PFL, HSP-20.

Introduction

Myocardial infarction (MI) is the main cause of death and also a major public health problem worldwide[1]. Early percutaneous coronary intervention (PCI) is currently the most effective treatment for MI[2,3]. However, continuous reperfusion after ischemia can usually cause secondary damage to the myocardium, which is called myocardial ischemia/reperfusion (I/R) injury[4]. I/R injury is an inevitable pathophysiological phenomenon in the treatment of ischemic heart disease and heart surgery in patients with thoracotomy, which can lead to reperfusion arrhythmia, temporary mechanical dysfunction, myocardial stunning, and other pathological changes[5]. Therefore, inhibiting myocardial I/R injury is of great significance to the prevention and treatment of ischemic cardiomyopathy, especially MI.

Long non-coding ribonucleic acids (lncRNAs) refer to long-chain RNA molecules whose transcription length exceeds 200 nucleotide units[6]. Although lncRNAs themselves cannot encode the corresponding proteins in cells, they can regulate the expression of the corresponding target genes at various levels, such as (post-) transcriptional level and epigenetic modification, and ultimate-

Corresponding Author: Jun Shen, BM; e-mail: rdwk55@163.com

ly affect the occurrence and development of the disease[7,8]. As a member of the lncRNA family, PFL plays an important role in many diseases, including tumors, cardiovascular diseases, and endocrine diseases[9]. In mouse myocardial fibrosis and TGF-β-induced myocardial cell fibrosis models, the expression level of PFL is significantly increased, but after PFL is knocked out by adenovirus, mouse myocardial fibrosis is markedly suppressed, and the proliferation of cardiac fibroblasts and their phenotypic transformation ability to myofibroblasts are also inhibited. Liang et al[10] have found that PFL may promote cardiac fibrosis in a mechanism related to its endogenous competitive Let-7d. However, the role of PFL in myocardial I/R injury has not yet been reported.

In this work, the heart I/R model was established using rats with PFL knockdown genes. The effects of PFL knockdown on cardiac function, apoptosis of heart cells, and infarction area of the heart were detected, and the potential molecular mechanism of PFL affecting myocardial I/R injury was analyzed.

Materials and Methods

Grouping and Processing of Laboratory Animals

This investigation was appr[illegible]y the A[illegible] imal Ethics Committee of N[illegible]niversity Animal Center. A total of 6[illegible]e Spr[illegible]e-Dawley (SD) rats weighing [illegible].61±13[illegible] were divided into 3 groups us[illegible] ra[illegible] table, including Con[illegible] grou[illegible]), I/R group (n=20), IR + PFL [illegible]all interfe[illegible]RNA (siRNA) group (n=20). There were no statistical differences in basic data such as weeks of age and body weight among the three grou[illegible] Rats in I/R + PFL siRNA group w[illegible]je[illegible] with a certain amount of PFL si[illegible]As (4 mL/kg) through the tail vein. The [illegible]fic surgical method for the construction of the [illegible]odel: the rats in each group were ane[illegible]tized [illegible]aper-itoneal injection of 50 m[illegible] pentobarb[illegible] then, the cannula was i[illegible]ted int[illegible]he left c[illegible]id artery to measure[illegible] blood[illegible]ssure of rats. Electrocardiography[illegible]G)[illegible]he lin[illegible] two leads was used t[illegible]tect[illegible]art rat[illegible]e thorax in the fou[illegible]intercosta[illegible]e[illegible] opened, and the per[illegible]m was cut [illegible]expose the heart. Th[illegible]r descendin[illegible] coronary artery (LA[illegible] was li[illegible]at 2 mm above the left atrial [illegible]ndage by th[illegible] silk thread to induce isc[illegible] After ischemi[illegible]r 30 min, the silk t[illegible]d was loosened, followed by reperfusion for [illegible] Rats in Co[illegible]l group underwent the same [illegible]edure, but t[illegible]silk thread was not ligated. A[illegible]reperfusi[illegible]he rats were killed, and the myo[illegible] in the anterior wall of the left ventricle[illegible]e rats was removed. After that, the [illegible]lood was rinsed with normal saline, and then, it [illegible]ed in a refrigerator at -80°C for standby [illegible]pli[illegible]on (Figure 1).

Echocardiography (ECG) Detection

To detect the cardiac function of each group of rats, MyLab 30CV ultrasound system (Esaote, SPA, Genoa, Italy) and 10-MHz linear ultrasonic transducers were used to detect the echocardiogram of rats in each group. After the shaving of the hair in the anterior thoracic region of mice

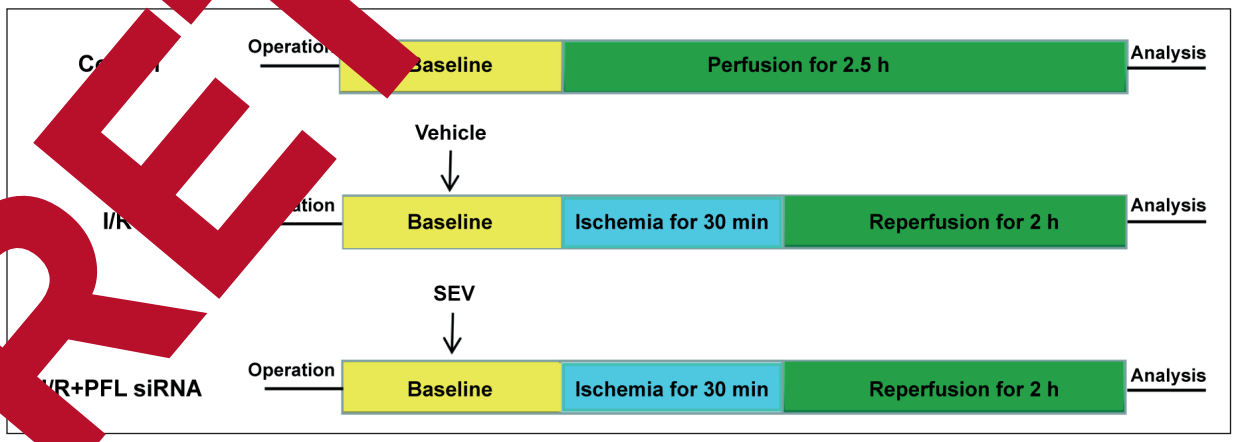

Figure 1. Flow charts of rat processing in each group. Control: Control group, I/R: I/R group; and I/R + PFL siRNA: I/R + PFL knockdown group.

and anesthesia, the mice were placed on a heating plate at 37°C with the left side facing up. Parameters including ejection fraction [EF (%)], fraction shortening [FS (%)], and heart rate (bpm) were detected.

Triphenyl Tetrazolium Chloride (TTC) Staining

1) Fresh brain tissues were put into a rat brain slice grinder and frozen in a refrigerator for 30 min at -20°C for slicing. 2) The brain tissue was cut into slices with a thickness of about 2 mm and no more than 6 slices per tissue. 3) The cut slices were placed in fresh TTC solution (2%) and fully contacted the TTC solution for an incubation time of not less than 0.5 h. 4) After 0.5 h, the slices were taken out and fixed with 4% paraformaldehyde, followed by photographing.

Hematoxylin and Eosin (H&E) Staining

The hearts obtained in each group were placed in 10% formalin overnight, dehydrated and embedded in wax blocks. Subsequently, all myocardial tissues were cut into thin slices with a thickness of 5 μm, fixed on glass slides and for staining. According to the instructions, they were soaked in xylene, ethanol at gradient concentration and hematoxylin, and then sealed with resin. After drying in the air, observation and photographing were conducted under optical microscope. The morphology of myocardial cells, cardiac interstitium, and myofilaments was observed.

Terminal Deoxynucleotidyl Transferase dUTP Nick End Labeling (TUNEL) Staining

The cut myocardial tissues were sliced, baked in an oven at 60°C for 30 min, waxed with xylene (5 min × 3 times) and dehydrated with 100%, 95%, 70% ethanol, respectively, each for 3 times. Then, slices were incubated with protein kinase for half an hour. After washing with phosphate buffered saline (PBS), the TdT and luminescence-labeled solutions were added. After reaction for 1 h at 37°C, horseradish peroxidase was added for incubation at 37°C incubator for 1 h at 37°C. Subsequently, the sections reacted at room temperature for 10 min with DAB as the substrate. After the nucleus was stained with hematoxylin, photographing and counting could be carried out under the optical microscope.

Immunohistochemical Staining

The cut myocardial tissue sections were baked in an oven at 60°C for 30 min and then dewaxed with xylene (5 min × 3 times), followed by hydration with 100%, 95% and 70% ethanol, respectively for 3 times. The endogenous peroxidase activity was inhibited by 3% hydrogen peroxide methanol, and then, the tissues were sealed with sheep serum for 1 h. Antibodies against heat shock protein 20 (HSP20) were diluted at 1:200 (PBS) and incubated at 4°C overnight, followed by washing with PBS 3 times in a shaker. After the second antibody was added, the color was developed with diaminobenzidine. After the completion of color development, 6 sections were randomly selected from each group, and 5 fields of view were randomly selected from each sample, followed by photographing under 200× and 400× optical microscopes.

Western Blot and Detection

After the heart tissues of rats in each group were fully ground in PBS buffer, they were ultrasonically lysed. The lysis buffer was centrifuged to extract supernatant, which was successively split into Eppendorf tubes (EP, Hamburg, Germany). The protein concentration was measured by the bicinchoninic acid (BCA) assay (Pierce, Rockford, IL, USA) and the ultraviolet spectrophotometry, and the protein volume of all samples was set to equal concentration. After subpackaging, the sections were placed in the refrigerator at -80°C. After the total protein was extracted, Sodium Dodecyl Sulphate-Polyacrylamide Gel Electrophoresis (SDS-PAGE) was performed. Then, the protein in the gel was transferred to cellulose acetate (polyvinylidene difluoride, PVDF) membrane (Roche, Basel, Switzerland), incubated in the primary antibody at 4°C overnight, and incubated in the goat anti-rabbit secondary antibody for 1 h away from light. The protein bands were scanned and quantified using an Odyssey membrane sweeper, and glyceraldehyde 3-phosphate dehydrogenase (GAPDH) was used to correct the level of proteins to be tested.

Statistical Analysis

All the data were analyzed by Statistical Product and Service Solutions (SPSS) 22.0 software (IBM, Armonk, NY, USA). Measurement data were expressed as mean ± standard deviation, and the comparisons of data between two groups were conducted using the *t*-test. $p<0.05$ represented that the difference was statistically significant.

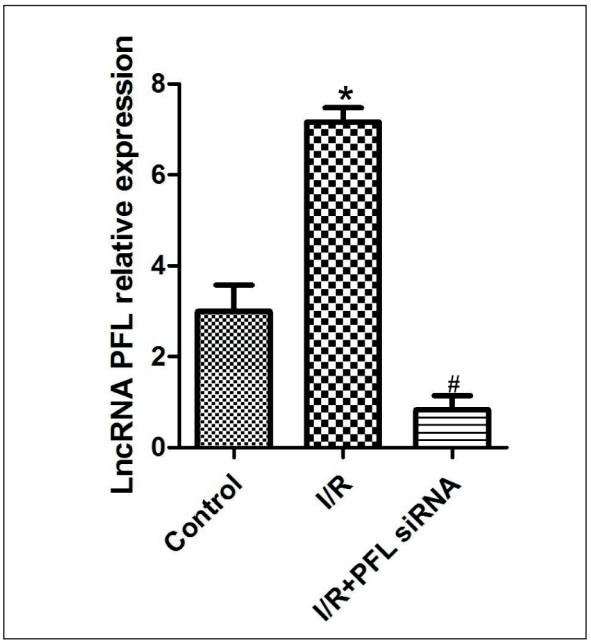

Figure 2. Expression of PFL in the myocardium of rats with I/R injury. Control: Control group, I/R: I/R group and I/R + PFL siRNA: I/R + PFL knockdown group. *p<0.05 *vs.* Control group and #p<0.05 *vs.* I/R group, displaying statistical differences.

Results

Expression of PFL in the Myocardium of Rats With I/R Injury

The expression level of PFL in the myocardium of rats in control group, I/R group and I/R + PFL siRNA group were detected respectively. The results showed that the expression level of PFL in I/R group was significantly increased (p<0.05), while it in rat myocardial tissues was significantly inhibited (p<0.05) after the injection of PFL siRNAs, indicating that the PFL knockdown model is successfully induced (Figure 2).

Effects of Knocking Down PFL on the Cardiac Function of Rats in Each Group

As shown in Figure 3, the ECG results manifested that there was no statistical difference in the heart rate among the groups of rats, so it could be excluded that the differences between EF (%) and FS (%) in each group was caused by the heart rate. Compared with rats in Control group, I/R rats had enlarged ventricular cavity and thickened cardiac wall, and PFL knockdown could obviously improve the abnormal changes in the cardiac structure caused by I/R. Furthermore, the levels of FS (%) and EF (%) in each group of rats were detected, which revealed that PFL knockdown markedly reversed the decreases in FS (%) and EF (%) in I/R group (p<0.05). The above results indicate that inhibiting PFL can improve the cardiac function of rats with I/R injury.

Knocking Down PFL Reduced the MI Area in I/R Rats

The heart infarction area in each group was evaluated by TTC staining. The results demonstrated that the infarction area of the three groups of rats were [(0.53±0.51) *vs.* (59.54±3.45) *vs.* (24.85±1.30)], with statistically significant differences (p<0.05), suggesting that the inhalation of

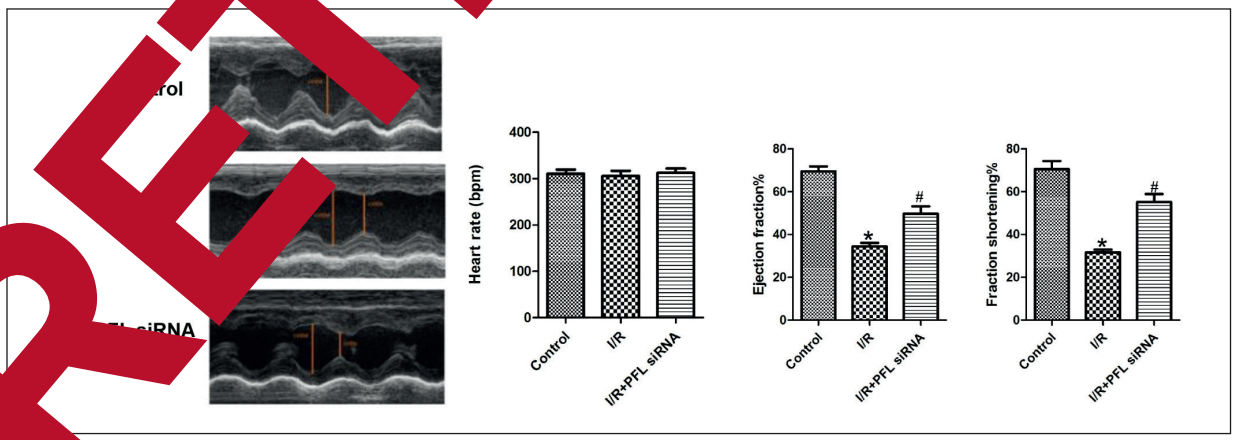

Figure 3. Effects of PFL knockdown on cardiac function of rats in each group. Control: Control group, I/R: I/R group and I/R + PFL siRNA: I/R + PFL knockdown group. *p<0.05 *vs.* Control group and #p<0.05 *vs.* I/R group, displaying statistical differences.

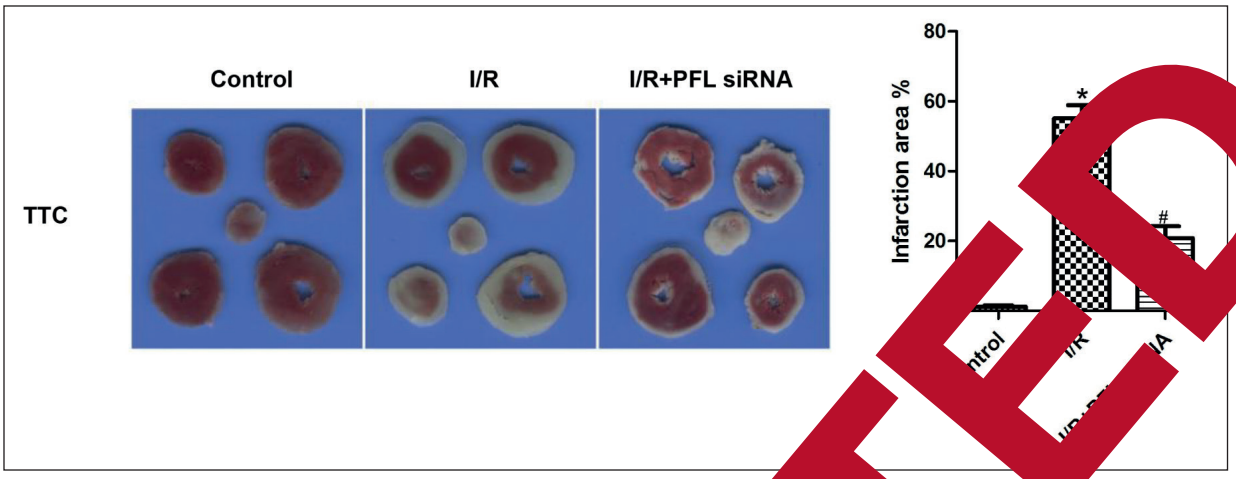

Figure 4. Effects of PFL knockdown on the MI area in each group of rats. Co... Co...up, I/R: I/R group and I/R + PFL siRNA: I/R + PFL knockdown group. *p<0.05 *vs.* Control group and #p<0.05 *vs.* I/R group, ...ving statistical differences.

PFL effectively reduces the MI area in I/R rats (Figure 4).

H&E Staining Results of the Heart of Rats in Each Group

To evaluate the changes in the myoc...ial cell microstructure in the heart cross se... rats in each group, H&E staining was perf...ed for myocardial tissues. According to the res... myocardial cells in I/R group showed evid... edema, disordered myofilamen...rangemen... degradation and necrosis t...degrees, accompanied by the infiltr...n of i...mmato-ry cells. However, after P... knockd...rats, the edema of the myoca...su... remarkably reduced, and t...ormality of myofilaments wa...o signifi...improved (Figure 5). The... results den...at PFL knockdown c...de... I/R-induced myocardial injury.

...cts of PFL Knockdown on ... Apoptosis ... Myocardial Cells in Rats

...Through TU... staining, the apoptosis lev-e... myocardia...ls in the three groups of rats was... results revealed that after I/R injury in..., the number of apoptotic myocardial cells was evidently increased (p<0.05), about ...42) times as much as that in the control ...oup, while after PFL knockdown, the number of apoptotic myocardial cells was decreased to (31.45±2.66) times as much as that in the control group (p<0.05) (Figure 6). The above results manifest that PFL knockdown can significantly inhibit the apoptosis of myocardial cells in rats.

Effects of PFL Knockdown on Genes Related to the Apoptosis of Myocardial Cells in Rats

Furthermore, the protein expression levels of apoptosis-related genes, Bcl-2-associated X protein

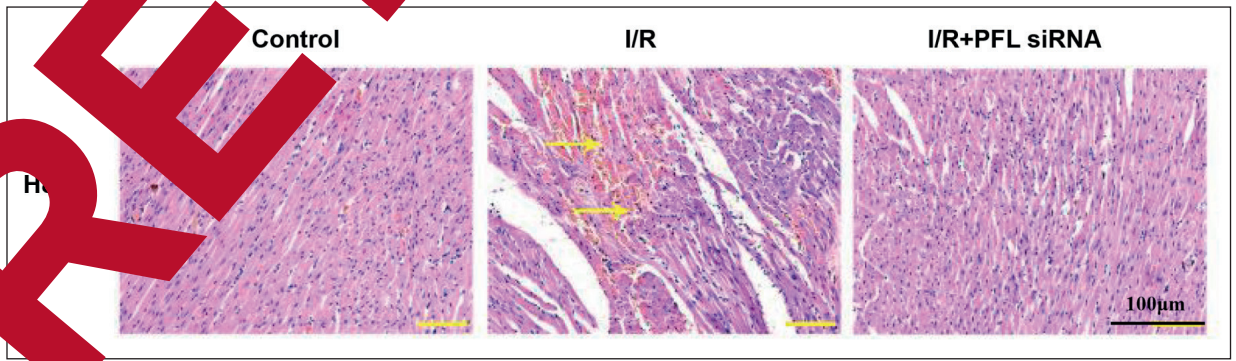

Figure 5. H&E staining results of the heart of rats in each group. Control: Control group, I/R: I/R group and I/R + PFL siRNA: I/R + PFL knockdown group.

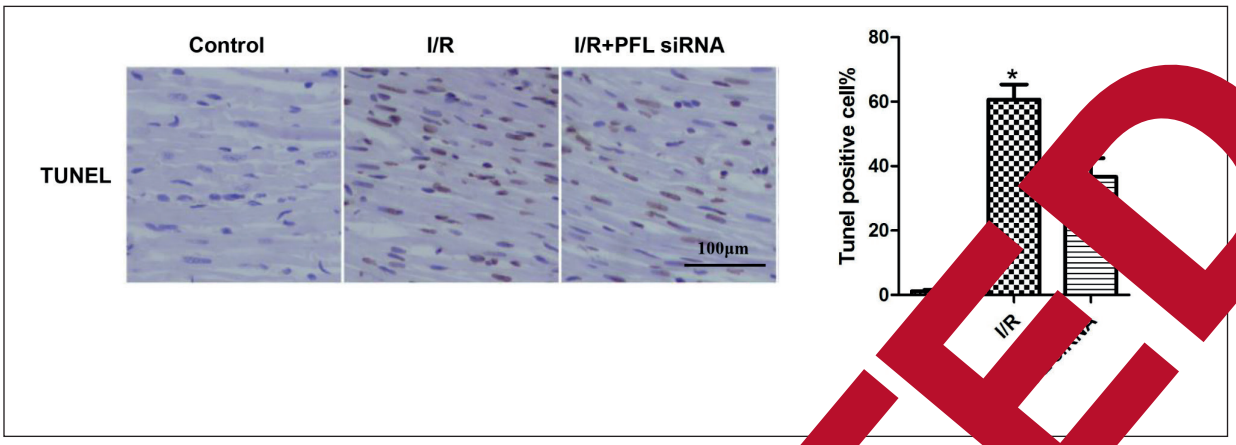

Figure 6. Effects of PFL knockdown on the apoptosis of myocardial cells in ea of rats. Contr ol group, I/R: I/R group and I/R + PFL siRNA: I/R + PFL knockdown group. *p<0.05 *vs.* C g and #p<0.05 *vs.* group, displaying statistical differences.

(BAX) and Bcl-2, in the myocardium of rats in each group were detected. The results demonstrated that the ratio of Bax/Bcl-2 in the myocardium of I/R rats was significantly increased, representing that the level of apoptosis was increased. Compared with that I/R group, the ratio of Bax/Bcl-2 in the myocardium of rats was decreased significantly in PFL siRNA group, further confirming the i ry effect of PFL siRNAs on the apoptosis of m r-dial cells caused by I/R injury (Figure 7).

Effects of Knocking Down P on HSP-20 in Each Grou

To investigate the effect PFL ckdown on myocardial I/R injury ts in d the ex-pression level of HSP-20 th

rat tected by imm istochemical stain- and Western blotting. According to the re- s, knocking n PFL could evidently reverse ow expressi f HSP-20 in the myocardium o caused b R injury (p<0.05) (Figure 8). The speculated that the myocardial protecti FL siRNA might be related to the tivation of HSP-20.

Discussion

Acute MI is still one of the most important causes of death worldwide[11]. Drug intervention (thrombolysis) or emergency PCI to rapidly restore blood flow through occluded coronary arteries is

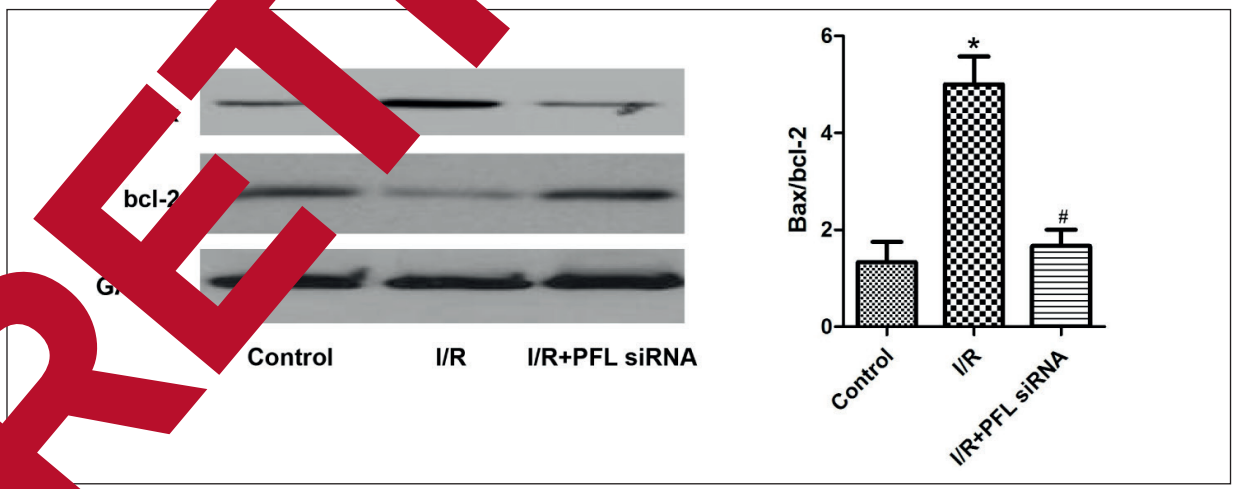

Fig 7. Effects of PFL knockdown on the expression of genes related to the apoptosis of myocardial cells in each group of rats. Control: Control group, I/R: I/R group and I/R + PFL siRNA: I/R + PFL knockdown group. *p<0.05 *vs.* Control group and #p<0.05 *vs.* I/R group, displaying statistical differences

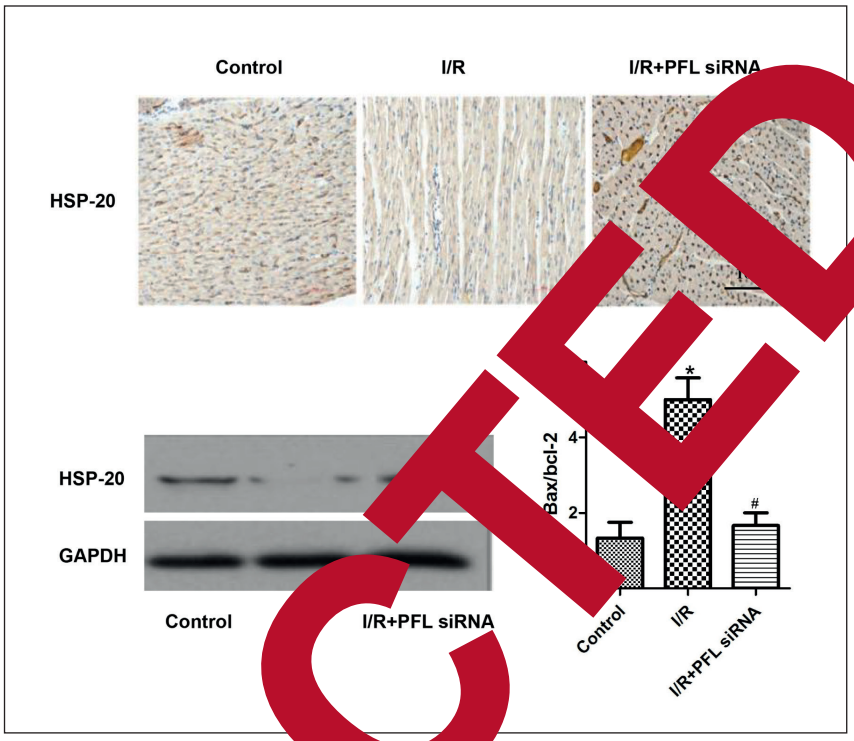

Figure 8. Effects of PFL knockdown on the expression of HSP-20 in heart tissues in each group of rats. Control: Control group, I/R: I/R group and I/R + PFL siRNA: I/R + PFL knockdown group. *p<0.05 *vs.* Control group and #p<0.05 *vs.* I/R group, displaying statistical differences

the most effective strategy to limit the [illegible] and improve the prognosis of patients after [illegible]te MI[12,13]. However, I/R itself can also lead to [illegible] tional myocardial cell death and further increase the infarction area of the heart. [illegible]rs leading to I/R injury mainly include [illegible]ress, inflammation, and apoptosis[14]. During [illegible]ocardial ischemia, adenosine triphosphate [illegible] in myocardial cells decrease[illegible] by the sarcoplasmic [illegible]culum, resulting in a large accumulation of Ca^{2+} in [illegible]chondria[15]. During reperfusion, re-entry of [illegible]en into myocardial cells will cause damage to the mitochondrial electron transport chain and increase the production of reactive oxygen species (ROS)[16]. Mitochondrial Ca^{2+} overload and increased ROS production both promote the opening of mitochondrial membrane permeability transformation pores, [illegible] in cell energy disorder and eventually irreversible cell [illegible]g necrosis and apoptosis[17,18]. [illegible], inhibiting myocardial cell apoptosis, inflammation, and oxidative stress during reperfusion can effectively improve cardiac [illegible] caused by I/R injury and reduce the infarction area of the heart.

HSP-20 is a lens protein originally found in the skeletal muscle, belonging to the HSP family[19]. Studies[20] have found that HSP-20 can improve the heat resistance of hamster ovary cells, and it can regulate blood vessel expansion and inhibit platelet aggregation. By transfecting adenovirus carrying HSP-20 into myocardial cells, the contractility of myocardial cells is significantly enhanced, and the apoptosis of myocardial cells induced by β-agonist is also significantly suppressed[21]. Furthermore, by selectively overexpressing HSP-20 in the myocardium, the cardiac function and cardiac injury in rats with I/R injury are markedly improved[22]. The mechanism of HSP-20 against myocardial I/R injury mainly includes 1) HSP-20 can regulate the ratio of Bax/Bcl-2, which tends to be stable, thus inhibiting cell apoptosis; 2) HSP-20 can form a stable complex with Bax, so as to inhibit Bax translocation from the cytoplasm to mitochondria, thus maintaining mitochondrial integrity and inhibiting Cytochrome C release and Caspase-3 activation; 3) HSP-20 can inhibit the injury of myofibrils during I/R and maintain the integrity of the myocardium. HSP-20 is transferred from the soluble part to the insoluble part of myocardial cells after I/R, so it can inhibit the collapse of intermediate silk-screen and prevent the damage of cytoskeleton protein. In this study, the tail vein injection of siRNAs was used to knock down PFL in heart tissues of rats by constructing a rat model of myocardial I/R injury. It was found that, when PFL was knocked down in rat myocardium, the decrease of cardiac function caused by I/R in-

jury was significantly improved, and the EF and FS were notably increased. Besides, PFL knockdown could also reduce the pathological damage to myocardial tissues of rats caused by I/R and maintain the integrity of muscle filaments in myocardial tissues. At the same time, PFL knockdown could also inhibit the level of apoptosis in myocardial tissues and the increase of Bax/Bcl-2 ratio caused by I/R. Finally, HSP-20, a protein closely related to MI occurrence in myocardial tissues of rats, was detected using Western blotting and immunohistochemical techniques. The results manifested that the HSP-20 level in the myocardium of rats was remarkably inhibited after I/R occurrence, but knocking down PFL could significantly reverse the decrease in HSP-20. Therefore, it was speculated that HSP-20 played an important role in the myocardial protection role of PSF siRNAs. Nevertheless, it was believed that there are still some limitations in this experiment: 1) Cell experiments were not designed for verification, and 2) the direct target of PFL was not found.

Conclusions

This study revealed for the first time th[illegible]FL plays an important role in myocardial I/R in[illegible]. Knocking down PFL can alleviate myocardial [illegible] injury by up-regulating the HSP[illegible]pression.

Conflict of Interests

The authors declare that th[illegible]

[illegible]nces

1) Agewal[illegible] Beltrame J[illegible]olds HR, Niessner A, Rosan[illegible] Caforio AL, De[illegible]na R, Zimarino M, Ro[illegible] Kjeldsen K, Atar D, [illegible]ski JC, Sechtem U, T[illegible]ll P. E[illegible] working group position paper on [illegible]cardial [illegible]ction with non-obstructive coro[illegible]rte[illegible] Eur He[illegible]J 2017; 38: 143-153.
2) H[illegible]ersh BJ[illegible] pathophysiology of acute myoc[illegible] infarc[illegible] and strategies of protection [illegible]yond [illegible]: a continual challenge. Eur [illegible]art J 20[illegible] 774-784.
3) [illegible]mholz HM, Hennen J, Ridker PM, Murillo JE, [illegible]rino V, Ellerbeck EF, Radford MJ. Use and [illegible]eness of intravenous heparin therapy for treatment of acute myocardial infarction in the elderly. J Am Coll Cardiol 1998; 31: 973-979.
[illegible]ao D, Yang J, Yang L. Insights for oxidative [illegible]ess and mTOR signaling in myocardial ischemia/reperfusion injury under diabetes. Oxid Med Cell Longev 2017; 2017: 6437467.
5) Chen Y, Ba L, Huang W, Liu Y, Pan H, Mingyao E, Shi P, Wang Y, Li S, Qi H, Sun H, Cao Y. Role of carvacrol in cardioprotection against my[illegible]dial ischemia/reperfusion injury in rats [illegible] tivation of MAPK/ERK and Akt/e[illegible] signa[illegible] pathways. Eur J Pharmacol 2017[illegible]: 90-100.
6) Chen WK, Yu XH, Yang W, Wang[illegible] WS, Yan YG, Zhang J, Wang WJ. LncRNAs: n[illegible]ers in intervertebral disc degenera[illegible]on and [illegible]rthritis. Cell Prolif 2017; 50: [illegible]
7) Yang Y, Chen L, Gu J, [illegible] H, Yuan J, L[illegible] G, Wang S, Wu Y, Y[illegible], Wang[illegible] Liu Y, [illegible] Luo G, Li Y, Hu L[illegible]X, Wa[illegible] Guo M, X[illegible], Xi J, Wang H, Zh[illegible] L[illegible] Recurr[illegible]ly deregulated lncR[illegible]s [illegible]ellular [illegible]noma. Nat Commu[illegible]17; 8: [illegible]
8) Li L, Wan[illegible] Zhang HS. [illegible]RI in a rat model [illegible]ardial infarct[illegible]r Rev Med Pharm[illegible]8; 22: 4332-4[illegible]0.
9) Leiseg[illegible] MS. L[illegible]onge: how the lncRNA PFL promotes cardiac [illegible]. Theranostics 2018; 8: [illegible]
1[illegible] [illegible], Pan Z, Zhao X, [illegible] L, Sun J, Su X, Xu C, Zhou Y, Zhao D, Xu B, Li X, Yang B, Lu Y, Shan H. LncRNA PF[illegible]ntributes to cardiac fibrosis by acting as a co[illegible]eting endogenous RNA of let-7d. Theranostics [illegible]8; 8: 1180-1194.
1[illegible] SD, [illegible]ogiannis NG. The biological basis [illegible]air after myocardial infarction: from infla[illegible]on to fibrosis. Circ Res 2016; 119: 91-112.
12) Wollert KC, Meyer GP, Muller-Ehmsen J, Tschope [illegible] Bonarjee V, Larsen AI, May AE, Empen K, Chori[illegible]ulos E, Tebbe U, Waltenberger J, Mahrholdt H, Ri[illegible]er B, Pirr J, Fischer D, Korf-Klingebiel M, Arseniev L, Heuft HG, Brinchmann JE, Messinger D, Hertenstein B, Ganser A, Katus HA, Felix SB, Gawaz MP, Dickstein K, Schultheiss HP, Ladage D, Greulich S, Bauersachs J. Intracoronary autologous bone marrow cell transfer after myocardial infarction: the BOOST-2 randomised placebo-controlled clinical trial. Eur Heart J 2017; 38: 2936-2943.
13) Arslan F, Bongartz L, Ten BJ, Jukema JW, Appelman Y, Liem AH, de Winter RJ, van T HA, Damman P. 2017 ESC guidelines for the management of acute myocardial infarction in patients presenting with ST-segment elevation: comments from the Dutch ACS working group. Neth Heart J 2018; 26: 417-421.
14) Li J, Dreyer RP, Li X, Du X, Downing NS, Li L, Zhang HB, Feng F, Guan WC, Xu X, Li SX, Lin ZQ, Masoudi FA, Spertus JA, Krumholz HM, Jiang LX. China patient-centered evaluative assessment of cardiac events prospective study of acute myocardial infarction: study design. Chin Med J (Engl) 2016; 129: 72-80.
15) Weng L, Jia S, Xu C, Ye J, Cao Y, Liu Y, Zheng M. Nogo-C regulates post myocardial infarction fibrosis through the interaction with ER Ca(2+) leakage channel Sec61alpha in mouse hearts. Cell Death Dis 2018; 9: 612.
16) Cui G, Xin Q, Tseng H, Hoi MP, Wang Y, Yang B, Choi I, Wang Y, Yuan R, Chen K, Cong W, Lee SM. A novel Ca(2+) current blocker promotes angiogenesis and cardiac healing after experimental myocardial infarction in mice. Pharmacol Res 2018; 134: 109-117.

17) Kronenbitter A, Funk F, Hackert K, Gorressen S, Glaser D, Boknik P, Poschmann G, Stuhler K, Isic M, Kruger M, Schmitt JP. Impaired Ca(2+) cycling of nonischemic myocytes contributes to sarcomere dysfunction early after myocardial infarction. J Mol Cell Cardiol 2018; 119: 28-39.
18) Javidanpour S, Dianat M, Badavi M, Mard SA. The cardioprotective effect of rosmarinic acid on acute myocardial infarction and genes involved in Ca(2+) homeostasis. Free Radic Res 2017; 51: 911-923.
19) Liu GS, Gardner G, Adly G, Jiang M, Cai WF, Lam CK, Alogaili F, Robbins N, Rubinstein J, Kranias EG. A novel human S10F-Hsp20 mutation induces lethal peripartum cardiomyopathy. J Cell Mol Med 2018:
20) Flynn CR, Komalavilas P, Tessier D, Thresher J, Niederkofler EE, Dreiza CM, Nelson RW, Panitch A, Joshi L, Brophy CM. Transduction of biologically active motifs of the small heat shock-rela HSP20 leads to relaxation of vas smo muscle. FASEB J 2003; 17: 1358 0.
21) Kozawa O, Matsuno H, Niwa M, yama D, Oiso Y, Kato K, Uematsu T. HSP20, low lar-weight heat shock-related protein acts ex larly as a regulator of platelet fu ns: a no nse mechanism. Life Sci 2 72: 113-124.
22) Fan GC, Ren X, Qian an Q, olaou P, Y, Jones WK, Chu G anias EG vel cardiopro-tective role of a s at-s protein Hsp20, against ische /re injury. lation 2005; 111: 1 799.